JOURNAL OF COMPUTATIONAL PHYSICS 15, 504–521 (1974)

Numerical Cherenkov Instabilities in Electromagnetic Particle Codes*

BRENDAN B. GODFREY

University of California, Los Alamos Scientific Laboratory, Los Alamos, New Mexico 87544

Received September 11, 1973; revised May 10, 1974

Linear dispersion relations for one-dimensional, electromagnetic particle simulation codes are analyzed in order to determine numerical stability properties. It is found that fast particles may resonate with light waves of matching phase velocity to produce a severe numerical instability. A Courant condition for this instability is derived, and comparison of its restrictiveness made among the various differencing schemes. At least two algorithms permitting reasonably large time steps for relativistic simulations are available.

1. INTRODUCTION

Over the past several years the utility of particle-in-cell computer simulation codes [1] in investigating highly complex plasma physics phenomena has been well established. Nonetheless, it must be remembered that, due to the approximations which must be made in a plasma simulation, the results obtained cannot be expected to reproduce actual plasma behavior in all detail. To quantify differences, various authors have developed a theory of "computer plasmas" [2, 3, 4] paralleling the basic features of ordinary plasma theory, and have performed detailed "computer experiments" [5, 6] to verify this theory. Such studies have done much to facilitate the efficient utilization of particle codes and the proper interpretation of their results.

With but few exceptions [7, 8], this theoretical analysis of particle codes has been restricted to electrostatic problems. In an attempt to alleviate this deficiency, we present the analysis of a simple yet significant numerical effect afflicting most relativistic electromagnetic particle codes. Specifically, we have found in a series of simulations that a cold, one-species plasma streaming rapidly in a spatially periodic, standard, one-dimension, electromagnetic particle code [9] gives rise to a rapidly growing numerical instability. Other simulations indicated that this same instability can arise in a variety of problems involving relativistic plasmas, including very hot

* This work performed under the auspices of the United States Atomic Energy Commission.

stationary Maxwellians. In all cases it is produced by an unphysical resonance between fast particles and electromagnetic waves of matching phase velocity. For this reason we refer to the effect as a numerical Cherenkov instability.

To better understand this behavior, we here derive and analyze in detail a linear dispersion relation, including all relevant numerical effects, for the simplest case possible, that of the cold beam just mentioned. This dispersion relation is sufficiently general to include most electromagnetic differencing schemes ordinarily used. Two less conventional schemes, advancing the fields in spatial Fourier-transform space and advancing the fields by advective differencing, are also studied. In all instances we find that, in addition to the usual high frequency light waves, the dispersion relation contains a ballistic (or beaming) mode, spurious in the sense that it does not exist in the limit of vanishing time step and cell size. It is the intersection of this mode with the light curves which occasions the numerical Cherenkov instability. On this basis it is straightforward to derive a Courant condition on particle motion. It states that, to avoid instability, particles can be moved no more than some fraction of a grid cell per time step, the precise distance depending on the differencing scheme used.

Study of the dispersion relation also provides the opportunity to gain added insight into the more usual Courant condition on the field equations. This is particularly fortunate in that the combination of particle and field Courant conditions can severely restrict the allowable time step for relativistic simulations, problems which in any event are quite expensive in computer time. A large portion of this paper is devoted to illustrating the ways in which reasonable time steps can be obtained. Our overall conclusion is that the numerical Cherenkov instability, while certainly a nuisance, can be avoided without excessive cost in computer time and apparently without undue violence to the physics to be simulated.

2. The Differencing Scheme

We begin by deriving the linear dispersion relation, including numerical effects, for a quite versatile but specific one space, three velocity electromagnetic particle code. Particle positions, charge density and electrostatic scalar potential, and electric and magnetic fields are known at integral time steps; particle velocities, current density and transverse vector potential at half-integral times. Fields are defined at cell edges, while potentials and charge and current densities are defined at cell centers (see Fig. 1). Standard area weighting is employed both for determining charge and current densities from particle positions and velocities and for determining the forces on particles from the fields defined on the (periodic) grid. All quantities are advanced using the leapfrog algorithm, space and time centered, and second-order accurate [1, 2].

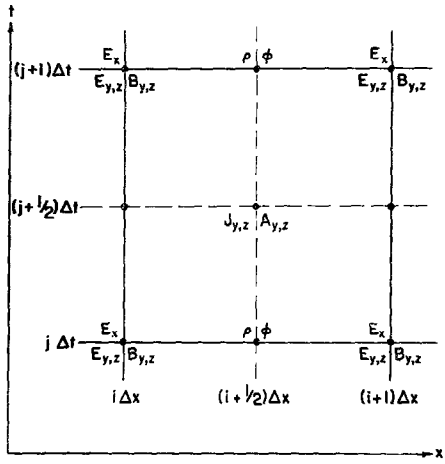

FIG. 1. Spacetime grid for the differencing scheme of Section 2.

Solution for the vector potential incorporates both multiple time steps [10] and implicit differencing [11]. For the former, the particles are advanced only every Nth time step (N an odd positive integer), so as to save computational time when treating nonrelativistic particles. Currents computed at the Nth time step are employed in advancing the vector potential also at the $L = (N - 1)/2$ time steps to either side. Typically, N is either one or three.

Implicit differencing involves modifying the vector potential equation to read

$$\frac{d^2}{dt^2}\left(1 + \beta\,\Delta x^2 \frac{d^2}{dx^2}\right)\mathbf{A} = \frac{d^2}{dx^2}\mathbf{A} + \mathbf{J}, \tag{1}$$

where Δx is the cell size and β is the implicitness parameter, $-\infty < \beta < 0.25$. (Units are chosen such that the plasma frequency and velocity of light each equal one.) As shown in Section 3, increasing β increases the phase velocity of light waves. For $\beta \leqslant -0.25\,(\Delta t/\Delta x)^2$, Δt the field time step, there is no Courant condition on the vector potential equation. Note that this technique can be applied with identical effect when the electromagnetic fields themselves are integrated forward in time (as in Ref. [10]):

$$(d/dt)(1 + \beta\,\Delta x^2(d^2/dx^2))\,\mathbf{E} = \nabla_x \times \mathbf{B} - \mathbf{J}, \qquad (d/dt)\,\mathbf{B} = -\nabla_x \times \mathbf{E}. \tag{2}$$

This decomposition of Eq. (1) is not necessarily unique.

Our derivation of the linearized, Fourier-transformed Vlasov equation proceeds just as in [2], except that we desire to know the first-order distribution function, f,

at half-integral rather than at integral times. As a consequence, tangent is replaced by sine in the usual expression:

$$f = i\mathbf{F} \cdot \frac{\partial f^0}{\partial \mathbf{v}} \Big/ \frac{\sin[(\omega + kv)\, N\Delta t/2]}{N\,\Delta t/2}. \tag{3}$$

This substitution represents one significant difference between electrostatic and electromagnetic dispersion relations. In Eq. (3), $\mathbf{F}$ is the total force as felt by the particles, f^0 is the zero-order distribution function, and ω and k are the frequency and wave number, respectively. Incidentally, even though Eq. (3) strictly is valid only non-relativistically, our final result is equally valid (with the usual mass renormalization) for a relativistic code, because we assume no thermal spread in f^0.

For a single cold beam in a charge neutralizing background, it is elementary to obtain from Eq. (3) the first-order current density.

$$\mathbf{J} = -\mathbf{A}\left[\frac{\sin(\omega\,\Delta t/2)}{\Delta t/2}\cos(k\,\Delta x/2) + v\,\frac{\sin(k\,\Delta x/2)}{\Delta x/2}\cos(\omega\,\Delta t/2)\right] \cdot \left[\frac{\sin(k\,\Delta x/2)}{k\,\Delta x/2}\right]^4 \Big/ \frac{\sin[(\omega + kv)\, N\,\Delta t/2]}{N\,\Delta t/2}. \tag{4}$$

This expression ignores spatial aliases [2] as comparatively unimportant for present purposes. To include them, replace k by $k + lk_g$ throughout the second line of Eq. (4) and sum on $l(k_g = 2\pi/\Delta x, -\infty < l < \infty)$.

Special care must be taken in Fourier transforming Eq. (1), that proper account is taken of the aliasing due to multiple time steps. The result is

$$\mathbf{A}_\omega\left[\left(\frac{\sin(\omega\,\Delta t/2)}{\Delta t/2}\right)^2\left(1 - 4\beta\sin^2(k\,\Delta x/2)\right) - \left(\frac{\sin(k\,\Delta x/2)}{\Delta x/2}\right)^2\right] = -\frac{\sin(\omega N\,\Delta t/2)}{N\sin(\omega\,\Delta t/2)}\sum_{l=-L}^{L}\mathbf{J}_{\omega+l\omega_g}, \tag{5}$$

with $\omega_g = 2\pi/N\,\Delta t$. The $\mathbf{N}$ homogeneous equations implicit in (4) and (5) are easily solved to yield the desired dispersion relation

$$1 = \left(\frac{\sin(k\,\Delta x/2)}{k\,\Delta x/2}\right)^4 \sum_{l=-L}^{L}\frac{\sin(\omega N\,\Delta t/2)}{\sin(\omega\,\Delta t/2 + l\pi/N)} \cdot \left[\frac{\sin(\omega\Delta t/2 + l\pi/N)\cos(k\Delta x/2) + (v\Delta t/\Delta x)\cos(\omega\Delta t/2 + l\pi/N)\sin(k\Delta x/2)}{\sin[(\omega + kv)\, N\,\Delta t/2]}\right] \Big/ \left[\left(\frac{\sin(\omega\,\Delta t + l\pi/N)}{\Delta t/2}\right)^2(1 - 4\beta\sin^2(k\,\Delta x/2)) - \left(\frac{\sin(k\,\Delta x/2)}{\Delta x/2}\right)^2\right]. \tag{6}$$

As previously mentioned, this expression is valid both relativistically and non-relativistically, and could have been obtained equally from Eq. (1) or Eq. (2).

3. Courant Conditions

A cursory examination of Eq. (6) indicates that it possesses not one but two sets of roots, corresponding to the high frequency light modes and, additionally, to a spurious beaming mode. Approximately,

$$\omega \approx \pm \frac{2}{\Delta t} \arcsin \left[\frac{\Delta t}{\Delta x} \frac{\sin(k\,\Delta x/2)}{[1 - 4\beta \sin^2(k\,\Delta x/2)]^{1/2}} \right] + l\omega_g \tag{7}$$

and

$$\omega \approx -kv + l\omega_g\,. \tag{8}$$

For reasonable accuracy, Eq. (7) requires $\Delta t < 1 < k$. If Δt is much greater than 1.5, the light modes are unstable near $k = 0$. A similar restriction on Δt, involving Langmuir waves, occurs in electrostatic simulations [12].

Figure 2 gives the exact solution to Eq. (6), determined numerically, for $N = 3$, $\beta = 0$, $v = 0.2$, $\Delta x = 0.1$, and $N\Delta t = 0.2$, in the range $0 < \omega < \omega_g$. The complete solution would consist of $3(N - 1)$ additional branches, corresponding to other l values in (7) and (8). (The simulation particles, with time step $N\Delta t$, see the various

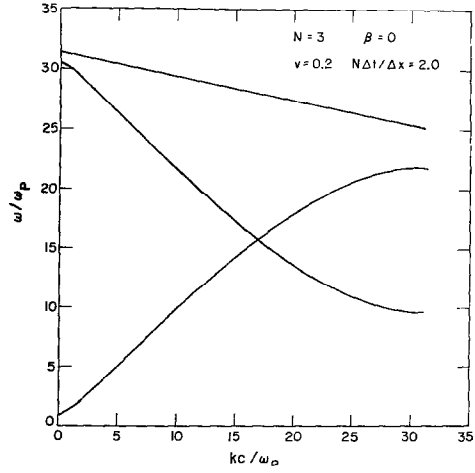

Fig. 2. Typical numerical solution of Eq. (6). Shown are two light wave and one beam branches. The two light modes are of different l, so that their intersection is stable.

time aliases as one.) Figure 3 is the power spectrum for $k = 0.98$, taken from a simulation performed with the parameters of Fig. 2. The three modes of Fig. 2 are prominent near the center of the diagram. Other modes, at higher frequencies and much lower intensities, arise from spatial aliases.

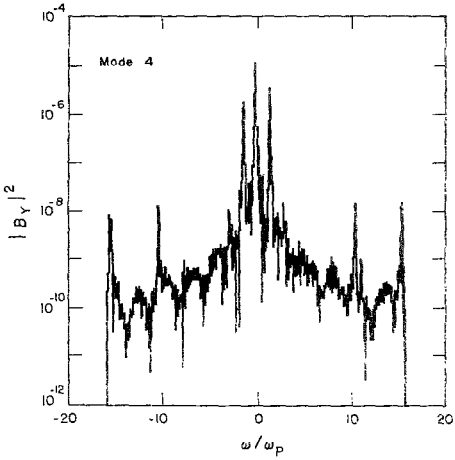

FIG. 3. Power spectrum for $k = 0.98$ from an electromagnetic particle code simulation; $N = 3$, $\beta = 0$, $v = 0.2$, $\Delta x = 0.1$, and $N\Delta t = 0.2$. Note the dominant beaming and light modes at $\omega = -0.2$ and ± 1.4, respectively.

When branches of (7) and (8) intersect in the $k - \omega$ plane, one should expect instabilities. There are three distinguishable cases: crossing of light modes with the same l value, crossing of light modes with different l values, and crossing of a light mode and a beam mode. To avoid the first possibility, require the argument of the arcsine in (7) not to exceed unity. Since the argument is largest for $k = k_{\max} = \pi/\Delta x$, we obtain

$$\Delta t \leqslant \Delta x(1 - 4\beta)^{1/2}, \tag{9}$$

i.e., the standard Courant condition, modified by implicit differencing. If this relation is violated, a well known virulent instability arises. The intersection of light branches of different l's (illustrated in Fig. 2) is, on the other hand, usually stable. Moreover, in the few exceptional cases, the instability grows slowly and is observed in computer simulations to saturate at an innocuous level.

The final case, intersection of a spurious beam mode and a light mode, typically leads to the powerful numerical Cherenkov instability described in Section 1. Figure 4 shows a case of such intersections. The associated instability growth rates

are ~0.5. Computer simulations performed to verify these predictions exhibited violent instability at the indicated values of k. Resulting energy nonconservation was severe.

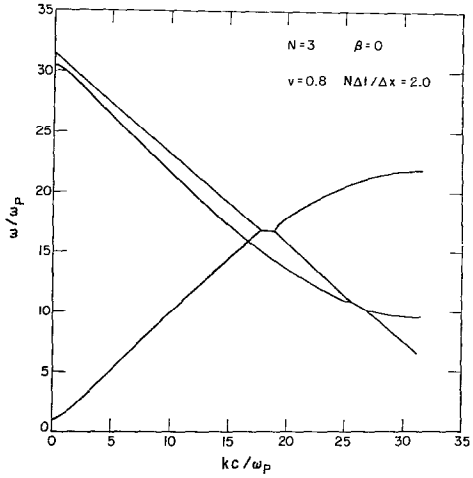

FIG. 4. Numerical solution of Eq. (6), illustrating numerical Cherenkov instabilities. Growth rates are of order 0.5.

Conditions sufficient for stability can be obtained by allowing the modes nearly to come together at $k_{\max}$. There are two inequalities of interest, for interaction of the beam mode with the nearest positive and negative [as defined by the sign in Eq. (7)] light modes, respectively.

$$v \leqslant \frac{2\,\Delta x}{N\,\Delta t}\left(1 - \frac{N}{\pi}\arcsin\left[\frac{\Delta t}{\Delta x}(1 - 4\beta)^{-1/2}\right]\right), \tag{10}$$

$$v \leqslant \frac{2\,\Delta x}{\pi\,\Delta t}\arcsin\left[\frac{\Delta t}{\Delta x}(1 - 4\beta)^{-1/2}\right]. \tag{11}$$

It cannot be emphasized too strongly that these relations are only approximate, and that, in particular, the second inequality is too weak when $N > 1$ and $v \cong 1$. Subject to this caveat, a second Courant condition can be obtained.

Equations (10) and (11) are most easily simultaneously satisfied when they are equivalent; i.e., when

$$\arcsin\left[(\Delta t/\Delta x)(1 - 4\beta)^{-1/2}\right] = \pi/2N. \tag{12}$$

In this case, one has simply

$$N\Delta t \leqslant \Delta x/v. \tag{13}$$

Thus, in distinction to electrostatic codes, in electromagnetic codes one cannot push particles faster than one cell per particle time step. The critical value of the implicitness parameter defined by Eq. (12) is

$$\beta_c = 0.25\,[1 - (\Delta t/\Delta x \sin(\pi/2N))^2]. \tag{14}$$

This is an exacting definition of β_c, particularly for $N = 1$, in that deviations from it of only a few percent may reduce the allowable particle time step dramatically. Note that β_c always satisfies Eq. (9).

The results, Eqs. (10)-(14) are, as derived, merely sufficient conditions for stability. To determine necessary conditions, we have expanded Eq. (6) about the frequency at intersection in order to find the sign of the coupling terms between the two modes. This computation, too lengthy to be reproduced here, indicates that, for parameters of practical interest, intersection always implies instability. Thus, Eqs. (10)-(14) are also necessary.

In a nonrelativistic problem, therefore, one could choose $N\Delta t = \Delta x/v$ and $\beta = \beta_c$ to obtain maximal computational speed. In practice one would back off slightly from each of these values, as they represent marginal stability. Other considerations, such as proper treatment of electrostatic phenomena, of course, bear upon the values chosen. The choice of N depends upon the user's tastes.

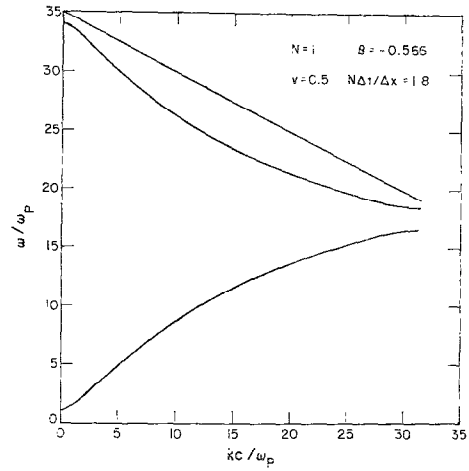

FIG. 5. Numerical solution of Eq. (6), showing effect of optimal choice of parameters for $N = 1$ and a nonrelativistic beam.

Figure 5 and 6 indicate typical contrasts. Recall that the light curves tangent at $k_{\max}$ in Fig. 6 are stable, since the modes are of different l's.

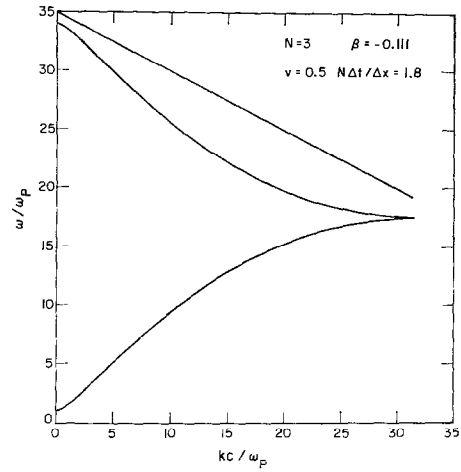

FIG. 6. Numerical solution of Eq. (6), showing effect of optimal choice of parameters for $N = 3$ and a nonrelativistic beam.

For relativistic velocities, the previous analytic approximations are less reliable, because the spurious beam mode and the negative light mode lie very near each other throughout their entire lengths. A numerical study of Eq. (6) was, therefore, performed using the ultra-relativistic limit $v = 1$. Results are unpromising. On the one hand, for $N > 1$, an instability occurs near $k_{\max}/4$ even with Eq. (13) and (14) satisfied. Slight adjustment in β together with a substantial reduction in Δt ameliorates the problem somewhat, but does not remove it. On the other hand, for $N = 1$ and β precisely equal to β_c, no instability occurs. Unfortunately, this is a condition of marginal stability according to Eq. (9). Thus, things otherwise minor in effect often can drive the system unstable. Indeed, when simulations were performed under these conditions ($N = 1, v = 1, \beta = \beta_c, \Delta t = 0.9\Delta x$), spatial aliasing led to a fast-growing instability. For $N = 1$ and $\beta < \beta_c$, instability arises near $k_{\max}/4$, just as for $N > 1$.

4. MODIFIED DISPERSION RELATIONS

Solutions to this apparent dilemma fall into two classes, arranging that the modes don't cross and arranging that crossing modes interact stably. A particularly simple approach of the first sort [13] is to increase the speed of light in the field equations (i.e., multiply Δt in Eq. (1) by some factor just greater than one) by enough that the negative light curve and the beaming curve no longer are tangent near $k_{\max}/4$. Since the fractional change required in the speed of light is small,

other stability conditions, Eqs. (9)–(14), would be relatively unchanged. Thus, at no additional computational effort, the numerical Cherenkov instability problem is solved even for highly relativistic beams. We have, however, not pursued this approach in detail, because a second appears less drastic yet equally effective.

Two groups [8, 11] have independently reported that defining the electric and magnetic fields on the same spatial mesh as the current density significantly reduces instability problems as compared with the staggered mesh scheme of Section 3. With this change Eq. (6) becomes

$$1 = \left(\frac{\sin(k\,\Delta x/2)}{k\,\Delta x/2}\right)^4 \sum_{l=-L}^{L} \frac{\sin(\omega N\,\Delta t/2)}{\sin(\omega\,\Delta t/2 + l\pi/N)} \cdot \left[\frac{\sin(\omega\Delta t/2 + l\pi/N) + (v\Delta t/\Delta x)\cos(\omega\Delta t/2 + l\pi/N)\sin(k\Delta x/2)\cos(k\Delta x/2)}{\sin[(\omega + kv)\,N\,\Delta t/2]}\right] \Big/ \left[\left(\frac{\sin(\omega\,\Delta t/2 + l\pi/N)}{\Delta t/2}\right)^2 (1 - 4\beta\sin^2(k\,\Delta x/2)) - \left(\frac{\sin(k\,\Delta x/2)}{\Delta x/2}\right)^2\right]. \quad (15)$$

Equations (7)–(14), derived from Eq. (6), clearly are unchanged. However, an analysis of the coupling between intersecting modes shows that the interaction of the negative light curve with the beaming curve is stable provided

$$\Delta t \leqslant 2\Delta x/v. \quad (16)$$

Intersection of the positive light mode with the beaming mode remains unconditionally unstable.

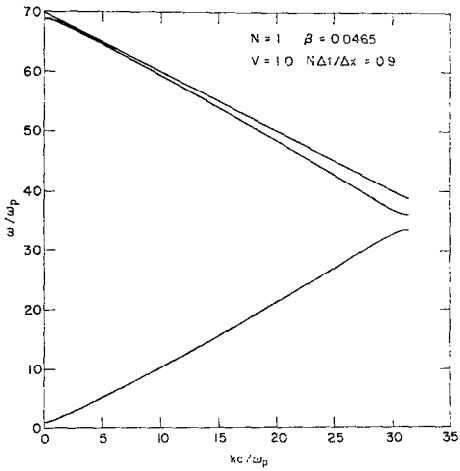

FIG. 7. Numerical solution of Eq. (15), showing effect of optimal choice of parameters for $N = 1$ and a relativistic beam.

Stability against the numerical Cherenkov instability, therefore, now requires (10) and (16) rather than (10) and (11). For very large β, Eq. (10) reduces to

$$N\Delta t \leqslant 2\Delta x/v, \tag{17}$$

which dominates Eq. (16). However, such a choice for β severely distorts the light wave dispersion. A physically more realistic choice is β just less than β_c, in which case Eq. (13) is recovered. Figure 7 provides a numerical solution to Eq. (15) for $N = 1$, $\beta = 0.98\beta_c$, $v = 1.0$, $\Delta x = 0.1$, and $\Delta t = 0.09$. Note that instability near $k_{\max}/4$ is no longer a problem.

5. Field Calculation by Fourier Transform

Next, we consider an unconventional method of determining the electromagnetic fields, namely by time integration of Maxwell's equations in Fourier transform space. With such an approach one hopes to adjust individually the dispersion of each mode in wavenumber space in such a way as to minimize the effects of finite differencing. In particular, one wishes to have for light waves $\omega = \pm k$ rather than, for instance, Eq. (7). As we shall see, even though the goal of dispersionless light curves is achieved only to first order, this field solving technique seems remarkably free of numerical limitations.

For definiteness let us analyze the algorithm of Haber *et al.* [14]. Others are similar [15]. For this differencing scheme field and particle quantities are defined on the space-time mesh as in Section 4; i.e., as in Fig. 1 (with, of course, $N = 1$) but with the fields defined on the same spatial mesh as the currents. Also as before, currents are determined by standard area weighting, as are the forces on the particles. However, transverse fields are advanced not as in Eq. (1) or (2) but by

$$\begin{aligned}
\mathbf{E}(t + \Delta t) &= \mathbf{E}(t)\cos(k\,\Delta t) + i\hat{\mathbf{k}} \times \mathbf{B}(t)\sin(k\,\Delta t) \\
&\quad - \frac{4\pi}{k} f\mathbf{J}\left(t + \frac{1}{2}\Delta t\right)\sin(k\,\Delta t), \\
\mathbf{B}(t + \Delta t) &= \mathbf{B}(t)\cos(k\,\Delta t) - i\hat{\mathbf{k}} \times \mathbf{E}(t)\sin(k\,\Delta t) \\
&\quad + \frac{4\pi i}{k} f\hat{\mathbf{k}} \times \mathbf{J}\left(t + \frac{1}{2}\Delta t\right)[1 - \cos(k\,\Delta t)].
\end{aligned} \tag{18}$$

where $\mathbf{E}$, $\mathbf{B}$, and $\mathbf{J}$ are to be understood as the $\mathbf{k}$th element of the spatially Fourier transformed fields and current density. $\hat{\mathbf{k}}$ is a unit vector along $\mathbf{k}$, which for our one-dimensional analysis points along the x axis. Finally, f is a form factor introduced to smooth the fields or to modify further their dispersion. Often,

$f = \exp[-k^2a^2]$ with $a \gtrsim \Delta x$ in order to suppress high frequency collisional effects.

Derivation from Eq. (18) of the cold beam dispersion relation proceeds as in Section 2, but more easily, since no multiple time steps are involved. The result is similar to Eq. (6), with the principle difference that Δx is replaced by Δt in most places.

$$\left(\frac{\sin(\omega\,\Delta t/2)}{\Delta t/2}\right)^2 - \left(\frac{\sin(k\,\Delta t/2)}{\Delta t/2}\right)^2 = \left(\frac{\sin(k\,\Delta x/2)}{k\,\Delta x/2}\right)^4 f \cdot \frac{\sin(k\,\Delta t/2)}{k\,\Delta t/2}\left[\frac{\sin(\omega\,\Delta t/2)\cos(k\,\Delta t/2) + v\cos(\omega\,\Delta t/2)\sin(k\,\Delta t/2)}{\sin[(\omega + kv)\,\Delta t/2]}\right] \tag{19}$$

Once again, spatial aliases have been ignored. To lowest order the normal modes are

$$\omega \approx \pm k, \tag{20}$$

$$\omega \approx -kv. \tag{21}$$

Note, however, that Eq. (20) requires $\Delta t < 1 < k$. Just as for Eq. (6) and Eq. (15), if Δt is greater than about 1.5, the light curves are unstable near $k = 0$. This constraint can be weakened somewhat by inserting the factor $[\sin(\Delta t/2)/(\Delta t/2)]^2$ into f. Even better choices of f for very large Δt are, of course, available.

If the plasma is absent, so that the right side of Eq. (19) vanishes, then Eq. (20) becomes exact, and there is no Courant condition on the light waves. However, the addition of plasma reactance just sufficiently distorts the light curves to cause instability where the modes intersect.

For ease of analysis, assume that $v = 0$. Then Eq. (19) reduces to

$$\sin^2(\omega\,\Delta t/2) = \sin^2(k\,\Delta t/2) + \left(\frac{\Delta t}{2}\right)^2\left(\frac{\sin(k\,\Delta x/2)}{k\,\Delta x/2}\right)^4 \cdot f\,\frac{\sin(k\,\Delta t)}{k\,\Delta t}. \tag{22}$$

Expand this expression about $k_t \equiv \pi/\Delta t$, the point of intersection of the light modes (actually of their time aliases).

$$\sin^2(\omega\,\Delta t/2) \approx 1 - \left(\frac{\pi}{2} - \frac{k\,\Delta t}{2}\right)^2 + \left(\frac{\pi}{2} - \frac{k\,\Delta t}{2}\right) g(k, \Delta t), \tag{23}$$

where g is shorthand for twice the coefficient of $\sin(k\,\Delta t)$ in Eq. (22). The right side of Eq. (23) attains a maximum of $1 + g^2/4$ at $\pi - k\,\Delta t = g$, giving a maximum instability growth rate $g/\Delta t$. The width of the instability region in k is

$$\Delta k/k_t \sim 2g/\pi. \tag{24}$$

One means of avoiding the instability is setting $k_{\max} \leqslant k_t(1 - 2g/\pi)$, i.e., satisfying the Courant condition

$$\Delta t \leqslant \Delta x(1 - 2g/\pi). \tag{25}$$

Since g typically is small near k_t, one usually has simply $\Delta t < \Delta x$. The second alternative is to arrange that the mode spacing in k, i.e., $2\pi/L$, where L is the length of the grid, exceeds the instability width defined in (24). This is best accomplished by choosing Δt not too large, say $\sim$0.2. It is, of course, equally possible to let Δt be large but make f small near k_t. However, one must be cautions, lest the physics of the problem be distorted.

When v is chosen not equal to zero, stability is more conveniently studied by numerical solution of Eq. (19). It is found that, although large v aggrevates somewhat the instability, the conclusions of the preceding two paragraphs remain approximately valid. Figure 8, with $f = 1$, $v = 0.6$, $\Delta x = 0.5$, and $\Delta t = 1.0$, is a particularly severe example. Growth rates for the intersection of the light modes are of order 0.2.

Also shown in Fig. 8 is the numerical Cherenkov instability due to intersection of the positive light curve with the beam curve. Growth rates are of order 0.4. For the present algorithm, this instability is particularly simple to investigate. The negative light mode and its aliases do not intersect the beam mode for parameters of practical interest. The positive light mode does not intersect the beam mode, provided

$$\Delta t \leqslant 2\,\Delta x/(1 + v). \tag{26}$$

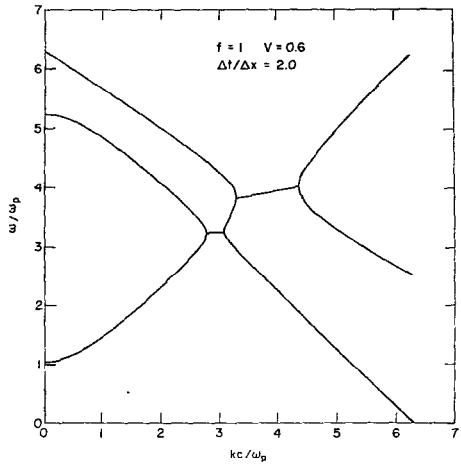

FIG. 8. Numerical solution of Eq. (19), illustrating effect of severe violation of both light and particle Courant conditions. Growth rates are of order 0.2 and 0.4, respectively.

An analysis of growth rates indicates that violation of (26) results always in instability. Figure 9, intentionally chosen as close as possible in parameters ($f = 1$, $v = 1.0$, $\Delta x = 0.1$, $\Delta t = 0.09$) to Fig. 7, illustrates stability even in the presence of an ultrarelativistic beam. Note that the beam mode and the negative light mode nearly coincide throughout their entire lengths.

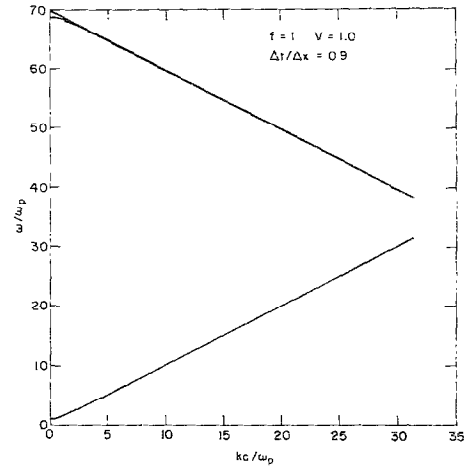

FIG. 9. Numerical solution of Eq. (19), illustrating optimal choice of parameters for $f = 1$ and a relativistic beam. Compare Fig. 7.

6. ADVECTIVE DIFFERENCING SCHEME

We conclude with an analysis of Langdon's advective differencing scheme [16]. Cast Maxwell's equations for E_y and B_z (similarly for E_z and B_y) into the form

$$\left(\frac{d}{dt} \pm \frac{d}{dx}\right)(E_y \pm B_z) = -J_y . \tag{27}$$

With the relevant quantities positioned on the space-time grid as in Fig. 1, the equations are differenced diagonally across the grid; i.e.,

$$(E_y \pm B_z)_{i\pm1,j+1} = (E_y \pm B_z)_{i,j} - (J_y)_{i+1/2,j+1/2}\,\Delta t. \tag{28}$$

Note that this requires $\Delta x = \Delta t$. If desired, one could define a separate, finer spatial mesh for treating the electrostatic field.

Now, the surprising thing about this scheme is that it is rigorously equivalent to a special case of the standard procedures described in Section 2, namely with $N = 1$, $\beta = 0$, and $\Delta x = \Delta t$. (This can be proven by straightforward manipulations of the corresponding finite difference equations.) Therefore, the improved stability attributed to codes using this scheme [16, 17] has, in fact, no connection with the field solving method. Rather, it is due to an unusual algorithm employed in determining the current.

Most codes compute currents at the half-integral time steps from particle velocities at that time and from positions obtained by averaging the positions of each particle from the preceding and following integral time steps. In the present instance, two separate currents are computed, one from the velocities at the half-integral time and the positions at the preceding integral time step and the other from the same velocities but with the positions at the following integral time step, and then averaged to obtain a current at the half-integral time. The effect of this alternate procedure is to modify the distribution function of Eq. (3) by the factor $\cos(kv\,\Delta t/2)$. The resulting dispersion relation follows immediately from Eq. (6).

$$\left(\frac{\sin(\omega\,\Delta t/2)}{\Delta t/2}\right)^2 - \left(\frac{\sin(k\,\Delta t/2)}{\Delta t/2}\right)^2 = \left(\frac{\sin(k\,\Delta t/2)}{k\,\Delta t/2}\right)^4 \cdot \cos(kv\,\Delta t/2)\,\frac{\sin(\omega\,\Delta t/2)\cos(k\,\Delta t/2) + v\cos(\omega\,\Delta t/2)\sin(k\,\Delta t/2)}{\sin[(\omega + kv)\,\Delta t/2]}. \tag{29}$$

For v near unity the right side of Eq. (29) is strongly suppressed at large k. Thus, we should expect the problems associated with marginal stability described in Sec. III to be markedly reduced. Indeed, numerical solutions of (29) and actual computer simulations [17] both demonstrate stability for practical values of Δt when $v \approx 1$. For v small the analysis of Section 5 with $\Delta x = \Delta t$ applies. Again, for reasonable simulation parameters numerical instabilities are absent.

Of course, this same procedure for determining the current could be included in any of the differencing schemes discussed, in all cases with some improvement in stability. However, one might legitimately ask how desirable is a strong k-space smoothing which depends on particle velocity. The v dependence can be removed simply by instead computing current in the standard fashion but at spatial cell edges, then averaging to the cell center. The smoothing now becomes $\cos(k\,\Delta x/2)$. However, the question of whether even this smoothing distorts too severely the physics remains unanswered. Clearly, for some problems such smoothing is acceptable, for others not. More practical experience is required for a reasonable evalution of current smoothing to avoid instabilities by either of the two techniques described in this section.

7. Conclusions

We have seen that finite differencing of the particle and transverse field equations of motion in electromagnetic particle plasma simulation codes gives rise to a spurious beaming mode. Additionally, the finite differencing distorts the dispersion of naturally occurring electromagnetic waves. It is well known that a Courant condition on the time step must be satisfied in order to avoid a numerical instability due to crossing of light modes. Here we have found that the intersection of a light curve with a spurious beaming curve may also lead to an instability, the numerical Cherenkov instability, and that to avoid this effect an additional Courant condition must be imposed. Basically, it states that simulation particles may not travel further than some fraction of a grid cell per time step.

Within the context of the present analysis, which ignores both thermal and aliasing effects, there are basically two practical differencing schemes for avoiding these instabilities. One can advance the transverse fields in Fourier-transform space, thereby minimizing distortion to light modes. Alternatively, one can add terms to the finite-differenced Maxwell's equations which guarantee that the phase velocity of light waves exceeds unity. In either case, the nonphysical resonance of fast particles with light waves leading to the numerical Cherenkov instability is eliminated. The two methods seem about equally effective, so the choice between them must be based on other considerations. Finally, smoothing of the currents in space or time increases stability. Extensive experience with this approach is lacking.

Two extensions to the present study suggest themselves. First, improved differencing schemes should be sought. Second, an analysis of existing schemes for the effects of spatial aliases and of finite temperatures is desirable.

The most ambitious goal in improving differencing schemes is to eliminate the beaming mode entirely. While difficult, such an advance is perhaps not impossible. Also valuable is the optimization of algorithms. For instance, one might consider replacing d^4/dx^2dt^2 by d^4/dx^4 in Eq. (1) to avoid having to invert a tridiagonal system at each time step [18]. The codes described in this article are all of a "momentum conserving" sort. Modifications to obtain "energy conserving" algorithms [3] should not prove difficult.

In electrostatic simulations, choice of a cell size significantly larger than the plasma Debye length leads to an instability associated with weakly damped alias modes. [4, 5]. Similarly, one should expect aliases instabilities in electromagnetic simulations when cell size exceeds the plasma magnetic skin depth, c/ω_p. Additionally, the intersection of alias modes can produce instabilities of the sort described in this article, though generally with smaller growth rates and saturation levels. Some evidence for Cherenkov instabilities induced by aliases is mentioned in Section 3. Generally, thermal velocity spreads have an ameliorating influence on instabilities, both physical and numerical. Whether this holds true of the

Cherenkov instability is, however, unclear, since a high energy tail can make the Courant condition more difficult to satisfy. (Even a stationary Maxwellian distribution can be unstable in this way.) It is evident that much useful work can be done along these lines.

ACKNOWLEDGMENTS

The author wishes to thank E. Lindman, C. Neilson, and D. Forslund for their encouragement and good advice. He is indebted also to I. Haber for useful discussions on Fourier transform solutions of the field equations, and to B. Cohen for performing stability tests on the advective differencing scheme.

REFERENCES

1. R. L. MORSE, in "Methods of Computational Physics," (B. Adler, S. Fernbach, and M. Rotenberg, Eds.), Vol. 9, p. 213, Academic Press, New York, 1970.
2. E. L. LINDMAN, *J. Comp. Phys.* **5** (1970), 13; A. B. LANGDON, *J. Comp. Phys.* **6** (1970), 247; A. B. LANGDON, in "Proceedings of the Fourth Conference on Numerical Simulation of Plasmas" (J. Boris and R. Shanny, Eds.), p. 467, Naval Research Laboratory, Washington, D.C., 1970.
3. H. R. LEWIS, in "Methods of Computational Physics" (B. Adler, S. Fernbach, and M. Rotenberg, Eds.), Vol. 9, p. 307, Academic Press, New York, 1970; A. B. LANGDON, *J. Comp. Phys.* **12** (1973), 247.
4. C. K. BIRDSALL, A. B. LANGDON, AND H. OKUDA, in "Methods of Computational Physics" (B. Adler, S. Fernbach, and M. Rotenberg, Eds.), Vol. 9, p. 241, Academic Press, New York, 1970; A. B. LANGDON AND C. K. BIRDSALL, *Phys. Fluids* **13** (1970), 2115; H. OKUDA AND C. BIRDSALL, *Phys. Fluids* **13** (1970), 2123.
5. H. OKUDA, *J. Comp. Phys.* **10** (1972), 475; H. OKUDA, *Phys. Fluids* **13** (1972), 1268.
6. J. M. DAWSON, R. SHANNY, AND T. J. BIRMINGHAM, *Phys. Fluids* **12** (1969), 687; B. B. GODFREY AND B. S. NEWBURGER, submitted to *Plas. Physics.*
7. A. B. LANGDON, *Phys. Fluids* **15** (1972), 1149.
8. J. P. BORIS AND R. LEE, *J. Comp. Phys.* **12** (1973), 131.
9. REL, the code used, is a highly modified version of EMI, described in D. W. Forslund, E. L. Lindman, R. W. Mitchell, and R. L. Morse, LA-DC-72-721, Los Alamos Scientific Laboratory, Los Alamos, N. M., 1972. See also B. B. Godfrey, C. E. Rhoades, and K. A. Taggart, AFWL-TR-72-47, Air Force Weapons Laboratory, Albuquerque, 1972, Ch. V.
10. J. P. BORIS, in "Proceedings of the Fourth Conference on Numerical Simulation of Plasmas" (J. P. Boris and R. Shanny, Eds.), p. 3, Naval Research Laboratory, Washington, D.C., 1970.
11. C. NEILSON AND E. LINDMAN, in "Abstracts: Sherwood Theoretical Meeting," University of Texas, Austin, 1973, paper D9; C. Neilson and E. Lindman, in "Proceedings of the Sixth Conference on Numerical Simulation of Plasmas," p. 148, Lawrence Berkeley Laboratory, Berkeley, paper E3, 1973.
12. A. B. LANGDON, unpublished.
13. C. W. NEILSON, private communication.
14. R. LEE, J. P. BORIS, AND I. HABER, *Bull. Amer. Phys. Soc.* **17** (1972), 1048; I. HABER, R. LEE, H. H. KLEIN AND J. P. BORIS, in "Proceedings of the Sixth Conference on Numerical Simulation of Plasma," p. 46, Lawrence Berkeley Laboratory, Berkeley, paper B3, 1973.

15. See, e.g., A. T. LIN, H. OKUDA, AND J. M. DAWSON, in "Proceedings of the Sixth Conference on Numerical Simulation of Plasmas," p. 141, Lawrence Berkeley Laboratory, Berkeley, paper E1, 1973.
16. D. NICHOLSON, B. COHEN, A. N. KAUFMAN, C. E. MAX, M. MOSTROM, AND A. B. LANGDON, *Bull. Amer. Phys. Soc.* **18** (1973), 1361; A. B. LANGDON, unpublished.
17. B. COHEN, private communication.
18. E. L. LINDMAN, private communication.